Analysis of Transverse Loading on a Beam Utilizing the Beltrami-Michell Equations

ABSTRACT

The stress field of a beam with a circular cross-section have been developed in the current work. One end of the beam is fixed while the other end is under traverse load at its center. The Beltrami-Michell compatibility equations were utilized to obtain coefficients in an assumed stress function which can be used to derive the stress field. To visualize the stress distribution in the beam, one can use MATLAB to generate surface plots and contour plots for the developed stress field. According to the plots, the maximum σ_{31} can be found at the center area of the cross-section while the minimum σ_{32} is captured at the same area. The maximum shear stress in the section occurs at points along the perimeter of the section. Moreover, the goal of this paper is to prove that any stress function with higher order terms always converge to the same stress solution for the beam utilizing lower order terms.

Keywords: Beam bending; circular cross-section; stress field.

1. INTRODUCTION

There are numerous places where bending can be seen in the world. For instance, pure bending can be seen in the bar of a typical barbell when it is held overhead by a weightlifter [1]. In engineering, bending is a concept widely used in the design of machine or structural components, such as beams and girders [1]. This makes the bending of materials the most common engineering design consideration. Engineers need to be able to understand why bending occurs and what materials can sustain in terms of a force that produces a bending moment. A bending moment is typically obtained when one end of an object is fixed, and the opposing end is a free end subjected to a load. Bending moments generate internal stresses in a material and hence it is important to quantify those for design purposes, e.g. for factor-of-safety calculations. Figure 1 displays a generic beam with the mentioned loading case.

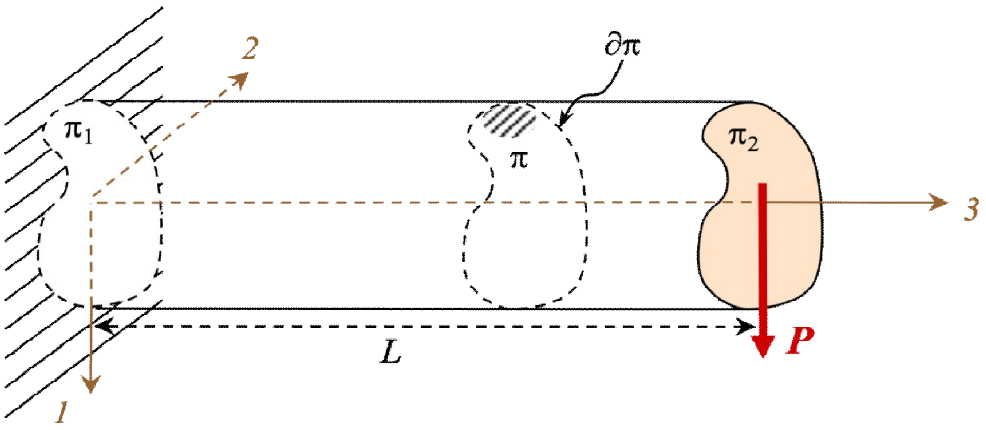

Fig. 1. General beam and loading schematic [2]

There are various loading conditions that can induce different bending moments. Some of these loading conditions can also create a twisting effect, or torsion. To simplify these conditions, this paper utilized one specific case. The beam is considered under the following specifications: (a) a transverse load is applied to the free end of the beam, (b) the transverse load is centered on the cross-section to not induce twisting, and (c) the cross-section is constant across the length of the beam. Beams with different cross-sections under transverse loading have been investigated by several researchers. The stress field of a beam with an elliptical cross-section was developed and presented in [3][4][5]. Study of a sandwich beam with a metallic foam core under transverse load was performed by Qin et al. [6]. Moreover, the bending collapse behavior of thin-walled square tubes was studied by Zhang et al. [7].

In this paper, a beam with a circular cross-section is focused on. Research on a beam with a circular cross-section has been done by [8][9][10]. In the current work, the stress field of a beam with a circular cross-section under (a), (b) and (c) conditions are developed. Additionally, this paper will showthat any assumed stress function will satisfy the Beltrami-Michell compatibility equations for a beam in bending.

2. METHODS AND MATHEMATICAL WORK

It is widely stated that the stress function solution is not vary based on the same geometry no matter the number of terms in the assumed solution; however, this has not been widely shown. This paper utilized Figure 2 for the cross-section dimensions and the following calculations. In addition, the beam has a length of *L*. The beam is fixed on the left side, whereas the right side is a free end with a centered transverse load. Furthermore, the terms x_1, x_2, and x_3 are used to signify the coordinate directions, also shown in Figure 2.

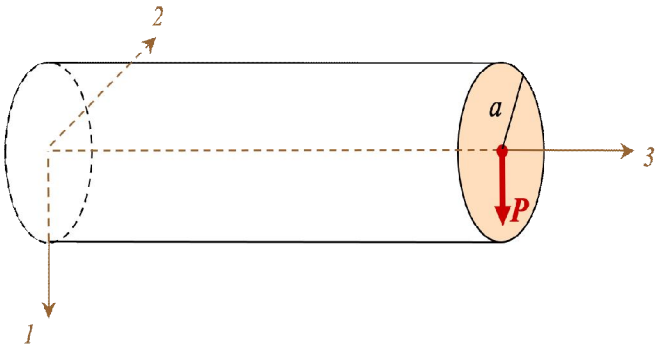

Fig. 2. Beam and loading schematic specific to this paper [2]

The governing equations that must be satisfied for beam bending are defined in Eq. (1) and (2). These two equations can be found by solving the Beltrami-Michell compatibility equations without including body forces:
[2].

$$\nabla^2 F = \frac{\upsilon}{1+\upsilon}\frac{P}{I}x_2 - 2\beta\mu \tag{1}$$

$$\frac{dF}{ds} = \frac{P}{2I}{x_1}^2\frac{dx_2}{ds} \tag{2}$$

In the second equation, *s* is a curvilinear length parameter along the perimeter of the cross-section. In this paper, the beam cross-section that is covered is a circle. Eq. (1) is defined for any generic cross-section. The $2\beta\mu$ term exists when the transverse load is not applied at the center of the beam, where β is the twist per unit length and μ is the shear modulus of the isotropic material. As this paper applies the load at the center of the cross-section, Eq. (1) can be simplified to [2]:

$$\nabla^2 F = \frac{\upsilon}{1+\upsilon}\frac{P}{I}x_2 \tag{3}$$

First, let's assume a solution of the form:

$$F = A{x_2}^3 + B{x_1}^2 x_2 + Cx_2 \tag{4}$$

To verify that the assumed solution is a valid solution, Eq. (4) must be substituted into the compatibility equations, Eq. (1) and (2), and the constants must be solved for. First, Eq. (4) is substituted into Eq. (3) to obtain the expression:

$$6Ax_2 + 2Bx_2 = \frac{\upsilon}{1+\upsilon}\frac{P}{I}x_2 \tag{5}$$

Eq. (5) only has x_2 as a common factor on both sides of the equation. This value can be factored out to create the first equation, Eq. (6), for the overall system of equations that are used to solve for the unknown constants:

$$6A + 2B = \frac{\upsilon}{1+\upsilon}\frac{P}{I} \quad (6)$$

Next, Eq. (4) must satisfy the second governing equation, Eq. (2). $\frac{dF}{ds}$ is a surface derivative of the cross-section. Surface derivatives are not easily found; however, it can be expanded using the chain rule [2]:

$$\frac{dF}{ds} = \frac{dF}{dx_1}\frac{dx_1}{ds} + \frac{dF}{dx_2}\frac{dx_2}{ds} \quad (7)$$

Now that the surface derivative has been expanded, Eq. (4) can be substituted into Eq. (7) in the $\frac{dF}{dx_1}$ and $\frac{dF}{dx_2}$ terms, creating Eq. (8):

$$\frac{dF}{ds} = (2Bx_1x_2)\frac{dx_1}{ds} + (3A{x_2}^2 + B{x_1}^2 + C)\frac{dx_2}{ds} \quad (8)$$

In Eq. (8), there are still two unknown derivatives. These can be derived based on the equation for the perimeter of the cross-section. On $\partial\pi$ (Figure 1), the perimeter equation is ${x_1}^2 + {x_2}^2 = a^2$. The last equation can be differentiated with respect to s. Using chain rule and solving for $\frac{dx_1}{ds}$, the following equation can be written [2]:

$$\frac{dx_1}{ds} = -\frac{x_2}{x_1}\frac{dx_2}{ds} \quad (9)$$

With this new relationship, Eq. (9) can be substituted into Eq. (8) to obtain (recall Eq. (2)):

$$(3A{x_2}^2 - 2B{x_2}^2 + B{x_1}^2 + C)\frac{dx_2}{ds} = \frac{P}{2I}{x_1}^2\frac{dx_2}{ds} \quad (10)$$

There are still numerous variable terms left in Eq. (10). Typically, it is easier to only work with one of the two directions, either x_1 or x_{22}. This allows for simpler substitution and less complex solutions. Since x_2 was already solved for earlier, the following derivations have x_2 as the only direction variable. x_1 can be found because the relationship between x_1 and x_2 is defined as ${x_1}^2 = a^2 - {x_2}^2$. This relationship is substituted into Eq. (10) to obtain:

$$(3A{x_2}^2 - 2B{x_2}^2 + B(a^2 - {x_2}^2) + C) = \frac{P}{2I}(a^2 - {x_2}^2) \quad (11)$$

To complete the system of equations, Eq. (11) needs to have its terms collected, Eq. (12). The upper line in Eq. (12) are the collected constant terms from Eq. (11), and the lower line in Eq. (12) are the x_2 terms from Eq. (11).

$$Ba^2 + C = \frac{P}{2I}a^2$$
$$3A - 3B = -\frac{P}{2I} \quad (12)$$

Using Eq. (6) and Eq. (12) as a system of equations, the solutions for *A*, *B*, and *C* are shown respectively as:

$$A = \frac{2\nu-1}{24(1+\nu)}\frac{P}{I}, \quad B = \frac{2\nu+1}{8(1+\nu)}\frac{P}{I}, \quad C = \frac{2\nu+3}{8(1+\nu)}\frac{P}{I}a^2 \qquad (13)$$

Eq. (4) is an assumed solution for this problem; however, this does not provide context for higher order terms or permutations of x_1 and x_2. Let's take a look at two additional terms. The terms Dx_1 and *E* are added to Eq. (4), to create the following equation:

$$F = Ax_2{}^3 + Bx_1{}^2x_2 + Cx_2 + Dx_1 + E \qquad (14)$$

Recall that Eq. (2) and (3) are the governing equations that must be satisfied. To obtain Eq. (15), Eq. (14) is substituted into Eq. (3).

$$\nabla^2 F = (6A + 2B)x_2 = \frac{\nu}{1+\nu}\frac{P}{I}x_2 \qquad (15)$$

Eq. (7) holds true for all boundary conditions because it is the chain rule expansion of $\frac{dF}{ds}$. Additionally, Eq. (9) holds true for a circular cross-section.

The same process are used as in the previous example. So, Eq. (9), Eq. (14), and $x_1{}^2 = a^2 - x_2{}^2$, are substituted into Eq. (7). Finally, by appropriately collecting the terms, the following relationships are found:

$$3A - 3B = -\frac{P}{2I}$$
$$Ba^2 + C = \frac{P}{2I}a^2$$
$$-D = 0 \qquad (16)$$

Combining Eq. (15) and Eq. (16) as a system of equations, the solutions of the system are determined in Eq. (17). This results in the same answers for *A*, *B*, and *C* as the Eq. (4) solutions. Additionally, the value of *E* does not matter in any of the solutions because it does not affect any of the solutions. Therefore, *E* is found to be 0.

$$A = \frac{2\nu-1}{24(1+\nu)}\frac{P}{I}, \quad B = \frac{2\nu+1}{8(1+\nu)}\frac{P}{I}, \quad C = \frac{2\nu+3}{8(1+\nu)}\frac{P}{I}a^2, \quad D = 0 \qquad (17)$$

Eq. (14) has 5 terms up to the third power for x_2 terms. However, higher order x_1 terms or various permutations have not been considered yet. The terms $Gx_1x_2{}^2$, $Hx_1{}^3$, $Jx_2{}^2$ and $Kx_1{}^2$ are added to Eq. (14) to create Eq. (18).

$$F = Ax_2{}^3 + Bx_1{}^2x_2 + Cx_2 + Dx_1 + E + Gx_1x_2{}^2 + Hx_1{}^3 + Jx_2{}^2 + Kx_1{}^2 \qquad (18)$$

Recall that Eq. (2) and (3) are the governing equations that must be satisfied. By substituting Eq. (18) into Eq. (3) and appropriately collecting terms, the simplified equation is:

$$\nabla^2 F = (6A + 2B)x_2 + (2G + 6H)x_1 + (2J + 2K) = \frac{\nu}{1+\nu}\frac{P}{I}x_2 \qquad (19)$$

By rewriting Eq. (19) as a system of equations, Eq. (20) is the found relationship. In Eq. (20), the first line is the x_2 terms, the second line is the x_1 terms, and the third line is the constant terms.$6A + 2B = \frac{\upsilon}{1+\upsilon}\frac{P}{I}$

$$2G + 6H = 0$$
$$2J + 2K = 0 \qquad (20)$$

The same process are used as the previous example. So, Eq. (9), Eq. (18), and ${x_1}^2 = a^2 - {x_2}^2$, are substituted into Eq. (7). Finally, by collecting terms appropriately, the following relationships are found:

$$3A - 3B = -\frac{P}{2I}$$
$$Ba^2 + C = \frac{P}{2I}a^2$$
$$D = 0$$
$$G = 0$$
$$2G - 3H = 0$$
$$2J - 2K = 0 \qquad (21)$$

By combining Eq. (20) and Eq. (21) as a system of equations, the solutions are determined in Eq. (22). This results in the same answers for *A*, *B*, and *C* as the Eq. (4) solutions. As mentioned earlier, the value of *E* does not matter in any of the solutions and is found to be 0.

$$A = \frac{2\nu-1}{24(1+\nu)}\frac{P}{I}, \qquad B = \frac{2\nu+1}{8(1+\nu)}\frac{P}{I}, \qquad C = \frac{2\nu+3}{8(1+\nu)}\frac{P}{I}a^2, \; D = G = H = J = K = 0 \quad (22)$$

Up to this point, this paper has covered permutations of x_1 and x_2 terms to the third power; however, there has not been a discussion on fourth power terms of x_1 and x_2. Adding ${Lx_1}^4$ and ${Mx_2}^4$ to Eq. (18) creates Eq. (23).
Note that this *L* coefficient in eq. (23) is different than the length *L* which is the length of the beam.

$$F = {Ax_2}^3 + {Bx_1}^2x_2 + Cx_2 + Dx_1 + E + Gx_1{x_2}^2 + {Hx_1}^3 + J{x_2}^2 + K{x_1}^2 + {Lx_1}^4 + {Mx_2}^4 \quad (23)$$

Recall that Eq. (2) and (3) are the governing equations that must be satisfied. By substituting Eq. (23) into Eq. (3), the obtained equation is:

$$\nabla^2 F = 12L{x_1}^2 + (2G + 6H)x_1 + (2J + 2K) + (6A + 2B)x_2 + 12M{x_2}^2 = \frac{\nu}{1+\nu}\frac{P}{I}x_2 \qquad (24)$$

By collecting the terms in Eq. (24), the following system is obtained:

$$12L = 0$$
$$(2G + 6H) = 0$$
$$(2J + 2K) = 0$$
$$(6A + 2B) = \frac{\nu}{1+\nu}\frac{P}{I}$$
$$12M = 0 \qquad (25)$$

As stated before, the same process are used from above. Eq. (9), Eq. (23), and ${x_1}^2 = a^2 - {x_2}^2$, are substituted into Eq. (7). Once again, we appropriately collect terms to obtain the following relationships:

$$3A - 3B = -\frac{P}{2I}$$
$$Ba^2 + C = \frac{P}{2I}a^2$$

$$-D - 3Ha^2 = 0$$
$$2G = 0$$
$$-G + 3H = 0$$
$$2J + 2K - 4La^2 = 0$$
$$4L + 4M = 0 \qquad (26)$$

By solving all these equations, Eq. (25) and Eq. (26) simultaneously, the solution obtained is Eq. (27). These solutions are the same answers for *A*, *B*, and *C* from all the various combinations shown above. In addition, the value of *E* does not matter in any of the solutions. Therefore, *E* is found to be 0.

$$A = \frac{2\nu-1}{24(1+\nu)}\frac{P}{I}, \qquad B = \frac{2\nu+1}{8(1+\nu)}\frac{P}{I}, \qquad C = \frac{2\nu+3}{8(1+\nu)}\frac{P}{I}a^2, \quad D = G = H = J = K = L = M = 0 \quad (27)$$

If this pattern was to continue for even higher terms and the multitude of permutations of the powers, the three terms (*A*, *B*, and *C*) always the same, and display the same stress function Eq. (28).

$$F = \frac{2\nu-1}{24(1+\nu)}\frac{P}{I}x_2{}^3 + \frac{2\nu+1}{8(1+\nu)}\frac{P}{I}x_1{}^2x_2 + \frac{2\nu+3}{8(1+\nu)}\frac{P}{I}a^2x_2 \qquad (28)$$

Let's consider the stress values at any given point in the circular beam. In general, the stress equations are defined in Eq. (29) (see reference [2]). In Eq. (29), *L* is the length of the beam, *P* is the applied force, and *I* is the second moment of inertia.

$$\sigma_{31} = F_{,2} - \frac{P}{2I}x_1{}^2$$
$$\sigma_{32} = -F_{,1}$$
$$\sigma_{33} = -\frac{P}{I}(L - x_3)x_1 \qquad (29)$$

From Eq. (28), it can be determined that the shear stresses σ_{31} and σ_{32} do not vary based on the length of the circular beam. However, the axial stress σ_{33} varied with the length. By substituting Eq. (28) into Eq. (29), the solution will provide equations that can be plotted (Eq. (30)). The following section will show the relevant plots using Eq. (30).

$$\sigma_{31} = \frac{3(2\nu-1)}{24(1+\nu)}\frac{P}{I}x_2{}^2 + \frac{2\nu+1}{8(1+\nu)}\frac{P}{I}x_1{}^2 + \frac{2\nu+3}{8(1+\nu)}\frac{P}{I}a^2 - \frac{P}{2I}x_1{}^2$$
$$\sigma_{32} = \frac{-2(2\nu+1)}{8(1+\nu)}\frac{P}{I}x_1x_2$$
$$\sigma_{33} = -\frac{P}{I}(L - x_3)x_1 \qquad (30)$$

The final results (equations (30)) match those in reference [2] and thus provide a verification for this work.

3. RESULTS AND DISCUSSION

Instead of normalizing the stress values with numerous variables, the following set of contour and surface plots used the parameter values in Eq. (31) to compute the stress values for σ_{31}, σ_{32}, and σ_{33}. These plots can be normalized by the radius, applied load, and Poisson ratio; however, this paper used select values for most of these variables.

a = 1 *meter,* P = 100 *N,* v = 0.3 (31)

The purpose of having both a contour plot and a surface plot is that a contour map is a 2-D representation of the stress field, whereas the surface plot is a 3-D representation of the stress field. Contour mapping displays the largest peaks for each of the sections but does not provide a smooth transition between points. A surface plot displays smooth transition between the plotted points.

Figures 3 and 4 display the stress field for σ_{31} in a contour map and surface plot, respectively; Figures 5 and 6 display the stress field for σ_{32} in a contour map and surface plot, respectively; and Figure 7 displays the stress field for σ_{33} in a contour map.

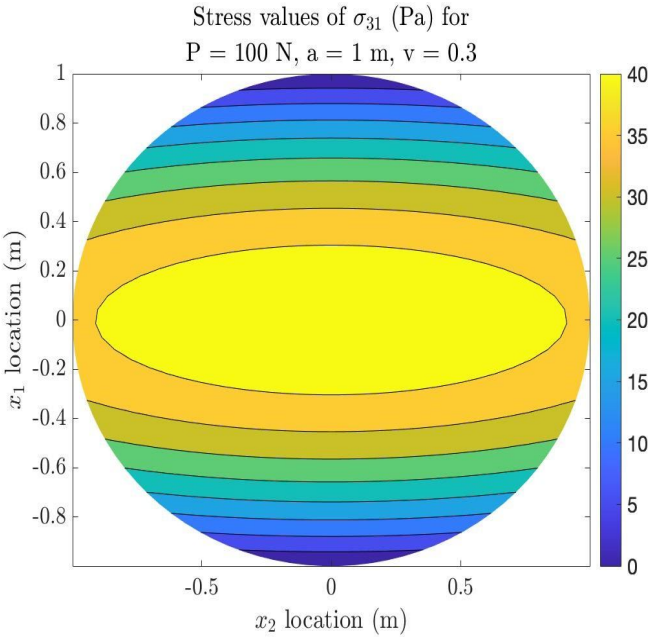

Fig. 3. σ_{31} Contour Plot

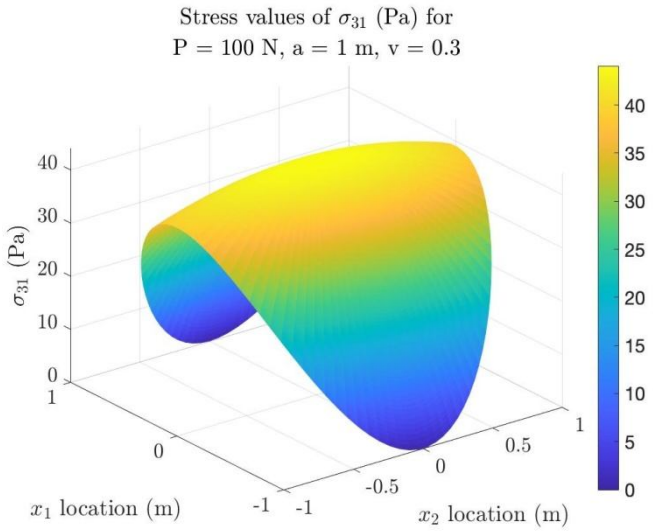

Fig. 4. σ_{31} Surface Plot

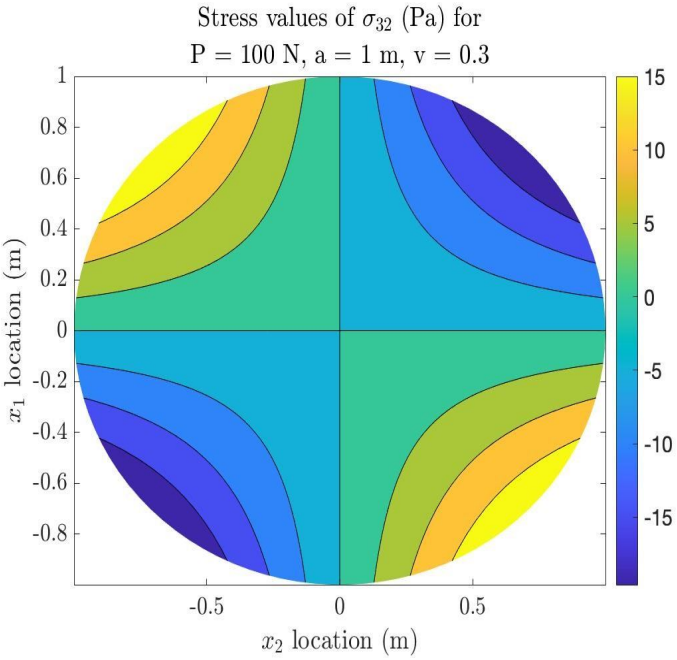

Fig. 5. σ_{32} Contour Plot

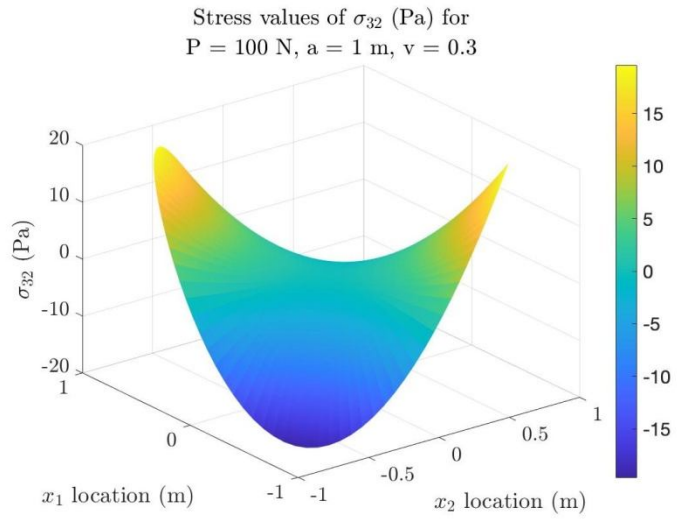

Fig. 6. σ_{32} Surface Plot

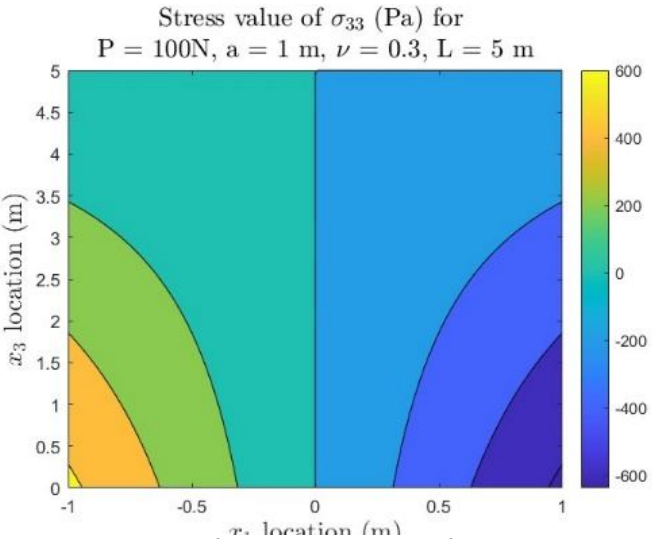

Fig. 7. σ_{33} Contour Plot

There are a few reasons for Figure 7 is not plotted in a circular view. The first is that the plot is of the x_1-x_3 plane, which is the side of the circular beam. This cross-section is when the beam is viewed from this direction. The second reason is that σ_{33} in Eq. (30) only depends on the x_1 and x_3 locations and not on x_2. The value of x_2 does not affect the final value of σ_{33}.

Finally, the most significant question that individuals thought of is: "How is the work completed in this paper verified?". The simplest way to verify the solution is to plot the vector field $\vec{\tau}$, Eq. (32). The work above is a valid solution if the vectors in the vector field plot are tangential to the perimeter of the cross-section and are zero at two locations: (a) $x_2 = 0$ and $x_1 = -1$, and (b) $x_2 = 0$ and $x_1 = 1$.

$$\vec{\tau} = \sigma_{31}\vec{\imath} + \sigma_{32}\vec{\jmath} \qquad (32)$$

The vector field for $\vec{\tau}$ is shown in Figure 8. As stated before, the vectors must be tangential at the perimeter of the cross-section. This is true for Figure 8. Also, the magnitude of $\vec{\tau}$ is zero at the above-mentioned two points (see Figure 8).

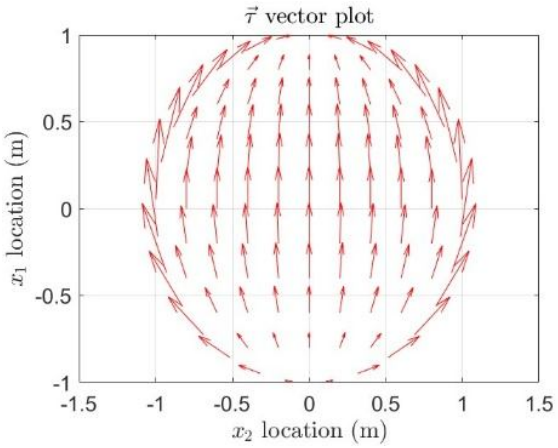

Fig. 8. $\vec{\tau}$ Vector Plot

It is important here to re-note the limitation of this work. The material is assumed to be isotropic here, and hence any anisotropy effects are not captured here. Also, there is no concurrent twisting of the beam with the described bending load.

4. CONCLUSIONS

This paper has determined that any stress function with numerous higher order terms always converge to the same classical solution for a circular cross-sectional beam in bending found in reference [2]. This was shown by utilizing the Beltrami-Michell formulas as the governing equations. Therefore, a limited number of terms in the stress function are required to reach this classical solution. It was also shown that the stress field for σ_{31} and σ_{32} can be considered as parabolic or bilinear in the x_1 and x_2 directions, whereas the stress field for σ_{33} is linear with the x_1 and x_3 directions. The developed stress field was verified by constructing the vector plot for $\vec{\tau}$ (the shearing vector in the cross-sectional plane). Finally, it can be determined that the magnitude of the stress values will vary based on the cross-section, loading magnitude, and the Poisson's ratio of the beam material.

COMPETING INTERESTS

Authors have declared that no competing interests exist.

AUTHOR'S CONTRIBUTIONS

This work was carried out in contribution among all authors. Author LL was responsible for resulting figures and reviewing. Author NG was responsible for the derivations, calculations, and resulting figures. Author TK reviewed this paper and served as an advisor during the research for this paper. All authors read and approved the final manuscript.

REFERENCES

[1] Beer FB, Johntson ER, DeWolf, JT, Mazurek DF. Mechanics of Materials. Sixth edition, TheMcGraw-Hill Companies, 2012.
[2] Khraishi TA, Shen YL. Introductory Continuum Mechanics with Applications to Elasticity (Revised Edition). Revised, Cognella Academic Pub, 2012.
[3] Roth S, Abuhegazy M, Khraishi TA. “Analysis of Beam Bending with an Elliptical Cross-Section,” Physical Science International Journal. 2021; 48–63. https://doi.org/10.9734/psij/2021/v25i630265
[4] Velazquez E, Kosmatka JB. "Stresses in a Half-Elliptic Curved Beam Subjected to Transverse Tip Forces," Journal of Applied Mechanics. 2012;80(1):2-6.
[5] Xu Z, Gardner L, Sadowski AJ. "Nonlinear stability of elastic elliptical cylindrical shells under uniform bending," International Journal of Mechanical Sciences. 2017;128–129:593-606.
[6] Qin QH, Wang T. “An analytical solution for the large deflections of a slender sandwich beam with a metallic foam core under transverse loading by a flat punch," Composite Structures. 2009;88(4):509- 518.
[7] Xiong Z, Hui Z, Zong W. “Bending collapse of square tube
with variable thickness,” International Journal of Mechanical Sciences. 2016; 106, 107-116, ISSN 0020-7403, https://doi.org/10.1016/j.ijmecsci.2015.12.006.
[8] Daunys M, Sergėjus R. “Analysis of circular cross-section element, loaded by static and cyclic elastic–plastic pure bending,” International Journal of Fatigue. 2006; 28: 211-222.
[9] Khalaf MS, Ibrahim AM, Najm HM, Hassan M, Sabri MM, Alamir MA, Alarifi M. “Evaluation and Prediction of the Bending Behavior of Circular Hollow Steel Tube Sections Using Finite Element Analysis. Materials,” 2022; 15. 3919.
[10] Feng R, Shen C, Lin J. “Finite-element analysis and design of aluminium alloy CHSs with circular through-holes in bending,” Thin-Walled Structures, Volume 144. 2019; 106289, ISSN 0263-8231, https://doi.org/10.1016/j.tws.2019.106289.